

Improved Limits on Spin-Dependent WIMP-Proton Interactions from a Two Liter CF₃I Bubble Chamber

E. Behnke,¹ J. Behnke,¹ S.J. Brice,² D. Broemmelsiek,² J.I. Collar,³ P.S. Cooper,²
M. Crisler,² C.E. Dahl,^{3,*} D. Fustin,³ J. Hall,^{2,†} J.H. Hinnefeld,¹ M. Hu,²
I. Levine,¹ E. Ramberg,² T. Shepherd,¹ A. Sonnenschein,² and M. Szydagis³

(COUPP Collaboration)

¹*Indiana University South Bend, South Bend, USA*

²*Fermi National Accelerator Laboratory, Batavia, USA*

³*Enrico Fermi Institute, KICP and Department of Physics, University of Chicago, Chicago, USA*

(Dated: October 17, 2018)

Data from the operation of a bubble chamber filled with 3.5 kg of CF₃I in a shallow underground site are reported. An analysis of ultrasound signals accompanying bubble nucleations confirms that alpha decays generate a significantly louder acoustic emission than single nuclear recoils, leading to an efficient background discrimination. Three dark matter candidate events were observed during an effective exposure of 28.1 kg-day, consistent with a neutron background. This observation provides strong direct detection constraints on WIMP-proton spin-dependent scattering for WIMP masses $> 20 \text{ GeV}/c^2$.

PACS numbers: 29.40.-n, 95.35.+d, 95.30.Cq, FERMILAB-PUB-10-318-A-CD-E

There is abundant evidence that $\sim 85\%$ of the matter in the Universe is cold, dark, and non-baryonic [1]. Together, dark matter and dark energy are pillars in modern cosmology which form a simple framework to understand the detailed observations of baryonic structure, the Hubble diagram, the cosmic microwave background, and the abundances of light elements. However, present knowledge of the nature of these essential ingredients of cosmology is limited. A new weak-scale symmetry, such as the preservation of R-parity in supersymmetry, would predict a massive particle with properties that conform with the current knowledge of dark matter [2]. If these Weakly Interacting Massive Particles (WIMPs) are the dark matter, then they may scatter off nuclei with enough energy, and at a high enough rate, to be detectable in the laboratory [3].

The Chicagoland Observatory for Underground Particle Physics (COUPP) employs the bubble chamber technique to search for WIMP-nucleon elastic scattering [4]. The bubble chamber is a powerful device to explore nuclear recoils in a rare event search. If the chamber pressure and temperature are chosen appropriately, electron recoils from the abundant gamma-ray and beta-decay backgrounds simply do not nucleate bubbles [5]. Neutrons from spontaneous fission and (alpha,n) in materials at the experimental site can be moderated with low-Z shielding materials, and cosmogenic neutrons can be reduced to negligible levels with an appropriate overburden. Due to the threshold nature of the bubble nucleation process, alpha-decays are more of a background concern for dark matter searches with superheated liq-

uids than they are for technologies with event-by-event energy measurements. Recently, however, the PICASSO collaboration reported event-by-event alpha-decay identification based on the acoustic emission from bubbles [6]. This letter confirms the observation of alpha discrimination and utilizes this technique to set limits on spin-dependent WIMP-proton scattering.

This letter reports results from a 3.5 kg CF₃I bubble chamber operated from August 19th to December 18th, 2009, in the MINOS near detector tunnel [7] at the Fermi National Accelerator Laboratory. The bubble chamber was located 3 meters off the axis of the NuMI neutrino beam [7], which operated with 10 μs pulses, typically every 2.5 seconds. The short duty factor allowed for a calibration source of efficiently tagged, beam-induced, fast neutrons. Additional calibration was provided using a switchable americium-beryllium neutron source (sAmBe) [5].

The 300 ft overburden of the NuMI site was sufficient to shield out the hadronic component of the cosmic ray flux and to significantly attenuate the cosmic ray muon flux. Residual cosmic ray muons passing near the bubble chamber were tagged using a 1000 gallon Bicron 517L liquid scintillator counter equipped with 19 RCA-2425 photomultiplier tubes which surrounded the experiment on the sides and above. The liquid scintillator, in conjunction with passive high-density polyethylene shielding below, provided a moderator for neutrons originating from natural radioactivity in the cavern rocks.

The bubble chamber consisted of a 150 mm diameter 3-liter synthetic fused silica [8] bell jar sealed to a flexible stainless steel bellows and immersed in propylene glycol within a stainless steel pressure vessel. The propylene glycol, which served as the hydraulic fluid to manage the inner pressure of the bubble chamber, was driven by an external pressure control unit. The flexible bellows

*Electronic address: cdahl@kicp.uchicago.edu

†Electronic address: jeter@fnal.gov

served to ensure that the contents of the bell jar were at the same pressure as the hydraulic fluid. The bell jar contained 3.5 kg of CF_3I topped with water. The water provided a buffer to ensure that the CF_3I contacted only the smooth silica and not the rough stainless steel surfaces.

The thermodynamic conditions of the chamber were monitored with two temperature sensors mounted on the bellows flanges and with three pressure transducers. Four lead zirconate piezoelectric acoustic transducers were epoxied to the exterior of the bell jar to record the acoustic emissions from bubble nucleations, the audible “plink” used to trigger the flash lamps in early bubble chambers [9]. Two VGA resolution CMOS cameras were used to photograph the chamber with a 20-degree stereo angle at a rate of 100 frames per second. Frame-to-frame differences in the image data provided the primary trigger for the experiment, typically initiating a compression within 20 ms of a bubble nucleation. Stereo image data from the cameras were used to reconstruct the spatial coordinates of each bubble within the chamber.

The chamber was operated at a temperature of 29.5°C and a pressure of 26.5 psia when sensitive to particle interactions, providing a Seitz model bubble nucleation threshold of 21 keV nuclear recoil energy [10]. Although this threshold depends on a theoretical model, it has been benchmarked by comparing to the threshold for sensitivity to alpha decays [5]. Reasonable uncertainties in the measurements of the thermodynamic state of the superheated target, about 1 psi and 0.5°C , correspond to a 15% shift in the threshold of the chamber and a 30% (15%) change in sensitivity for 50 (100) GeV WIMPs.

Following the nucleation of a bubble, the chamber was compressed to 215 psia for 30 seconds (300 seconds every 10th event) to re-condense the CF_3I vapor. During the compression period, data from the bubble event were logged, and the chamber was prepared for the next expansion. To allow for equilibration of the bubble chamber fluid, the valid live time for the chamber began 30 seconds after an expansion. From the outset, the performance of this chamber was a significant improvement over previous COUPP bubble chambers [5]. There was no evidence of radon beyond a few dozen events immediately after the chamber fill. Vessel wall nucleations due to alpha decays, observed at a rate of 0.7 events $\text{cm}^{-2} \text{day}^{-1}$ in natural quartz vessels, were at an unmeasurably low level in this synthetic fused silica vessel.

The data presented in this letter confirm PICASSO’s observation of a difference between the acoustic emissions from bubbles nucleated by nuclear recoils and bubbles nucleated by alpha decays [6]. The current understanding of the physics behind this discrimination is that the ultrasonic acoustic emission from a growing bubble peaks when the bubble is larger than a nuclear recoil track, tens of nanometers, but smaller than an alpha track, tens of microns [11]. At the time of peak acoustic emission, a nuclear recoil track is a single bubble, while an alpha track may contain several microscopic bubbles making the al-

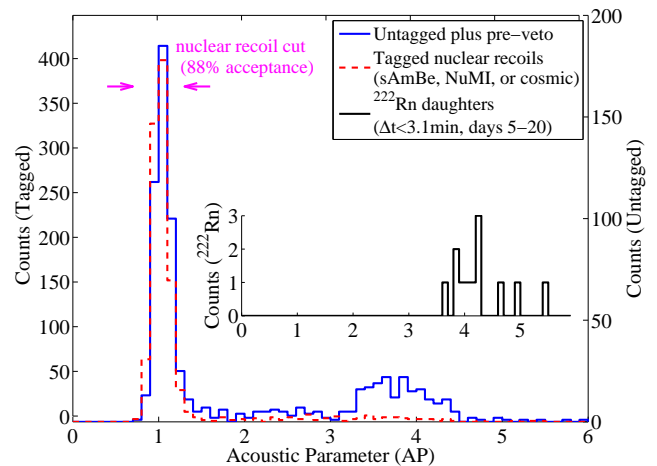


FIG. 1: The acoustic parameter, defined in the text, is a measure of the loudness of the acoustic “plink” resulting from bubble nucleations. The red, dashed histogram in the main panel is from the nuclear recoil calibration datasets (sAmBe, NuMI, cosmic). The blue, solid histogram in the main panel is from all the untagged data, including data taken before the muon veto was commissioned. The inset histogram contains events from ^{222}Rn early in the run, which reproduce the second peak in the untagged dataset. The acceptance of the nuclear recoil cut, indicated with arrows, is 88%.

pha event louder. Because the COUPP bubble chamber fluid is a homogeneous medium, it is expected that acoustic alpha/nuclear recoil discrimination should be more distinct than in the aqueous gel emulsion of superheated droplets used by PICASSO.

The acoustic transducer signals were digitized with a 2.5 MHz sampling rate and recorded for 100 ms for each event. The sound of bubble nucleation showed a broad emission distinctly above background noise up to a frequency of 200 kHz. The analysis of these signals was based on an acoustic parameter (AP) which is a measure of loudness. The AP is a frequency weighted acoustic power density integral, corrected for sensor gain and bubble position¹. The AP was scaled to have a value of unity at the peak observed in its distribution for bubbles induced by known neutron sources (the sAmBe source, the pulsed NuMI beam, or cosmic muons). The AP distribution from these known neutron sources is shown in

¹ $AP = \sum_j G_j \sum_n C_n(\vec{x}) \sum_{f_{min}^n}^{f_{max}^n} f \times psd_f^j$. $C_n(\vec{x})$ are corrections for the position dependence of the bubble acoustic emission. \vec{x} is the position of the bubble calculated from the stereoscopic images. G_j is the gain factor for acoustic transducer j . f is frequency, $n = 1 \dots 3$ indicates three frequency bands (5-30 kHz, 30-80 kHz, or 80-120 kHz), j identifies the acoustic sensor, f_{min} and f_{max} are the boundaries of the frequency band, and psd_f^j is the power spectral density for the bin with center frequency f for sensor j .

Fig. 1. Also shown is the distribution of untagged data, mostly the ~ 300 kg-day exposure before the scintillator veto was installed, which showed a peak at $AP = 1$ similar to the calibration data, with an additional component with $3 \leq AP \leq 5$. The low AP peak in the untagged data is caused by nuclear recoils and the higher AP peak is understood to be caused by alpha decays.

All data have been subject to a fiducial volume cut requiring the stereoscopically reconstructed bubble positions to be at least 5 mm away from the wall. The acceptance of this fiducial volume cut was 75% for nuclear recoils from the sAmBe and NuMI calibration samples. The definition of AP and of the AP cut were specified before the veto was installed, and neither was tuned based on the WIMP search data sample. The nuclear recoil acceptance of the AP cut was measured to be 88% in the fiducial volume using the NuMI coincident and sAmBe calibration events.

There was no viable method of injecting alpha-emitting isotopes into this bubble chamber. On the contrary, efforts were focused on removing these from the active volume, achieving a rate of $\simeq 0.7$ alpha decays per kg day. A small amount of ^{222}Rn injected during the fill of the chamber was identifiable via its characteristic decay time. These events were selected by requiring a time difference between bubbles of < 3 minutes, corresponding to the sequence of alpha decays from ^{222}Rn decaying to ^{218}Po ($T_{1/2} = 3.1$ min) which then emits a second alpha particle. This small sample of 10 known alpha decay events shown in the inset of Fig. 1 is consistent with the peaks observed in the untagged data at $3 \leq AP \leq 5$, confirming the expectation of a louder alpha acoustic emission.

The camera images and the slow pressure rise associated with bubble expansion provided two methods to count macroscopic bubbles in an event. These bubble counting methods were used to produce Fig. 2, where the AP is plotted as a function of bubble number inferred from the pressure rise. The symbols indicate how many bubbles were inferred from camera images. WIMP interactions will nucleate only one bubble. Neutrons are the only significant background able to produce multiple macroscopic bubbles during an event. The AP scales with the number of macroscopic bubbles. Tails in the AP distribution for a given number of macroscopic bubbles are all towards louder values.² This is consistent with the AP scaling linearly with acoustic energy, with a minimum acoustic energy produced by single bubbles.

Previous COUPP calibration data taken at 30°C showed that neutron induced nuclear recoils with energy above the Seitz threshold had a 50% chance of nucleating bubbles [5]. A comparison of MCNP simulations of

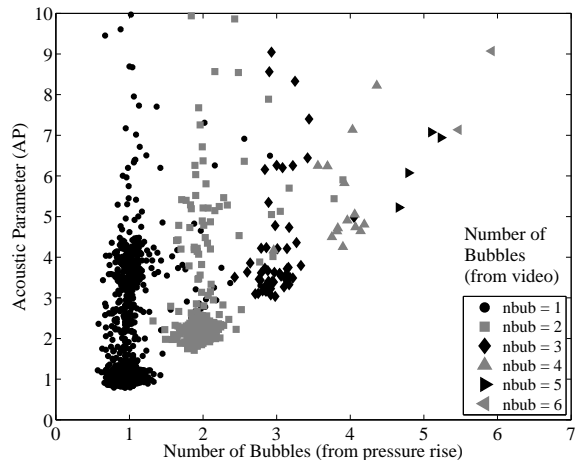


FIG. 2: The two methods of measuring the bubble multiplicity are plotted for the full data set of 291 kg-day exposure. The first method, based on automated video reconstruction software, searches for clusters of pixels changing between frames and is represented by the various symbols labeled in the legend. The second method of counting bubbles was to measure the dP/dt associated with an event. The abscissa is the pressure rise, scaled to the number of bubbles. The ordinate is the acoustic parameter AP (see text).

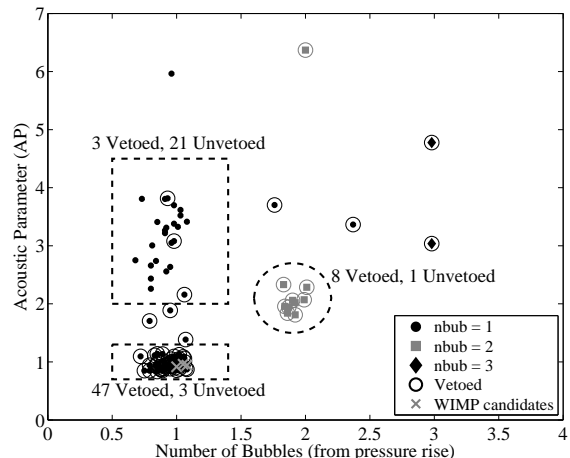


FIG. 3: Data from a 28.1 kg-day WIMP search, plotted as in Fig. 2. In the alpha region (large dashed box) 21 events with no evidence for muon activity were observed, with 3 events having coincident muon activity (labeled vetoed). The smaller dashed box indicates the WIMP signal region, containing 3 candidate events and 47 events coincident with muons in the veto. The neutron double scatter region, indicated with a dashed circle, contains 8 vetoed events and 1 unvetoed event, the latter indicating an irreducible neutron background contamination (see text).

² The high AP tails are a possible indication of inefficiency for the AP neutron selection, but not a background concern. The nature of the events in the tail of the acoustic parameter has not been studied. The rate is consistent with the expected rate of (n,alpha) reactions on fluorine and carbon.

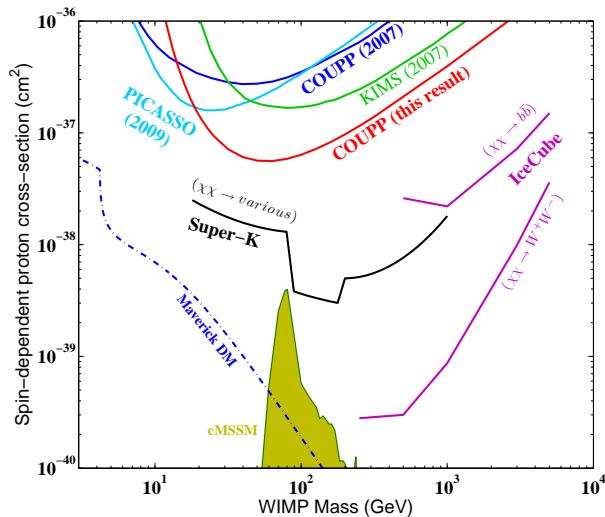


FIG. 4: Improved limits on spin-dependent WIMP-proton elastic scattering from the data presented in this letter. A previous COUPP result [5] is shown for comparison. Direct detection limits from the PICASSO experiment [12], cyan, and the KIMS experiment [13], green, are shown. Limits on neutralino annihilation in the Sun from the IceCube [15], magenta, and Super Kamiokande [14], black, neutrino observatories are also plotted. The indirect detection limits from the neutrino observations have additional dependence on the branching fractions of the annihilation products. The gold region indicates favored regions in cMSSM [16]. The blue, dashed-dotted line is the expected cross-section for “maverick” dark matter with $\Omega h^2 = 0.1$ [17].

single and multiple rates with the rates observed during sAmBe calibration is consistent with this 50% efficiency for the data presented here. The efficiency is expected to reach 100% at higher operating temperatures [5]; unfortunately, a mechanical failure forced an early termination of the run, restricting data-taking to 30°C.

The WIMP search data spanned November 19th to December 18th. They are shown in Fig. 3 along with the signal acceptance regions for various classes of event. There were 23 days of livetime with the muon veto active. A number of data quality cuts were imposed to remove periods of poor detector performance. The most restrictive data quality cut was imposed to excise intermittent noise on the acoustic signals, removing 42% of the science run. An effective exposure of 28.1 kg-days remained after imposing all data quality cuts, the fiducial volume cut, and the AP nuclear recoil cut. In the signal acceptance region there were 3 WIMP candidate events and 47 events coincident with muon activity in the veto. In the alpha region there were 24 events, 3 of which were coincident with muon activity. These are statistically consistent with the high- AP tail expected from the 47 cosmic ray events in the signal region. Of 9 events

with two macroscopic bubbles, one was not coincident with the veto. This event is proof of an unvetted neutron background component with sufficient rate to result in the observed 3 single-scatter WIMP candidate events.

Assessments of event-by-event discrimination against alpha decays and of the sensitivity to WIMP-nucleon scattering are limited by the unvetted neutron background in this dataset. Interpreting the three events in the signal region as alpha decays results in a conservative 90% C.L. upper limit on the binomial probability of an alpha decay registering in the nuclear recoil signal region of $< 26\%$. At this operating pressure and temperature, an alpha particle will create bubble nucleation sites along its entire track, and there is clear evidence of a neutron background from the multiple scatter events, so these three events are likely not alpha decays. Therefore the presently derived alpha background rejection should be considered a conservative assessment for the potential of this technique. We expect an improved estimate from runs in a deeper underground site, where the residual neutron background should be absent.

Interpreting the three events in the signal region as WIMP candidates results in a 90% Poisson upper limit of 6.7 for the mean of the signal. The resulting improved limits on spin-dependent WIMP-proton couplings are shown in Fig. 4. The spin-independent sensitivity that can be extracted from present data is comparable to that obtained by CDMS in another shallow underground facility [18]. The calculations assume the standard halo parameterization [19], with $\rho_D = 0.3 \text{ GeV c}^{-2} \text{ cm}^{-3}$, $v_{esc} = 650 \text{ km/s}$, $v_E = 244 \text{ km/s}$, $v_0 = 230 \text{ km/s}$, and the spin-dependent couplings from the compilation in Tovey *et al.*[20]. This result is consistent with a background from neutrons induced by residual cosmic radiation in the shallow site.

In view of the $\sim 10^{-11}$ intrinsic rejection against minimum ionizing backgrounds [5] and the acoustic alpha rejection demonstrated in this letter, a leading sensitivity to both spin-dependent and -independent WIMP couplings can be expected from the operation of CF_3I bubble chambers deep underground. A first exploration of the cMSSM spin-dependent parameter space [16] of supersymmetric dark matter candidates is expected from operation of this chamber in a deeper site. At the time of this writing, a 60 kg CF_3I COUPP bubble chamber is being commissioned.

The COUPP collaboration would like to thank Fermi National Accelerator Laboratory, the Department of Energy and the National Science Foundation for their support including grants PHY-0856273, PHY-0555472, PHY-0937500 and PHY-0919526. We acknowledge technical assistance from Fermilab’s Computing, Particle Physics, and Accelerator Divisions, and from E. Greiner, P. Marks, B. Sweeney, and A. Vollrath at IUSB.

-
- [1] E. Komatsu *et al.*, *Astroph. J. Suppl.* **180**, 330 (2009) and refs. therein.
- [2] G. Bertone, D. Hooper, and J. Silk., *Phys. Rep.* **405**, 279, (2005); J.L. Feng, to appear in *Ann. Rev. Astr. Astroph.*, [arXiv:1003.0904](https://arxiv.org/abs/1003.0904).
- [3] M.W. Goodman and E. Witten, *Phys. Rev.* **D31**, 3059 (1985).
- [4] W.J. Bolte *et al.*, *Nucl. Instr. Meth.* **A 577**, 569 (2007).
- [5] E. Behnke *et al.*, *Science* **319**, 933 (2008).
- [6] F. Aubin *et al.*, *New J. Phys.* **10**, 103017 (2008).
- [7] D.G. Michael *et al.*, *Nucl. Instr. Meth.* **A 596**, 190 (2008).
- [8] SUPRASIL manufactured by the Heraeus corporation.
- [9] D.A. Glaser and D.C. Rahm, *Phys. Rev.* **97**, 474 (1955).
- [10] F. Seitz, *Phys. Fluids* **1**, 2 (1958).
- [11] Y.N. Martynyuk *et al.*, *Sov. Phys. Acoust.* **37**, 376 (1991).
- [12] S. Archambault *et al.*, *Phys. Lett.* **B 682**, 185 (2009).
- [13] H.S. Lee *et al.*, *Phys. Rev. Lett.* **99**, 091301 (2007).
- [14] S. Desai *et al.*, *Phys. Rev.* **D 70**, 083523 (2004).
- [15] R. Abbasi *et al.*, *Phys. Rev. Lett.* **102**, 201302 (2009).
- [16] L. Roszkowski, R.R. de Austri, and R. Trotta, *JHEP* **0707**, 075 (2007).
- [17] M. Beltran, D. Hooper, E.W. Kolb, and Z.A.C. Krusberg, *Phys. Rev.* **D 80**, 043509 (2009); M. Beltran *et al.*, *JHEP* **1009**, 037 (2010).
- [18] D.S. Akerib *et al.*, *Phys. Rev.* **D 68**, 082002 (2003).
- [19] J.D. Lewin and P.F. Smith, *Astrop. Phys.* **6**, 87 (1996).
- [20] D.R. Tovey *et al.*, *Phys. Lett* **B 488**, 17 (2000).